STEM CELLS®

TRANSLATIONAL AND CLINICAL RESEARCH

In Vivo Interleukin-13-Primed Macrophages Contribute to Reduced Alloantigen-Specific T Cell Activation and Prolong Immunological Survival of Allogeneic Mesenchymal Stem Cell Implants

CHLOÉ J. HOORNAERT,[a,b] EVI LUYCKX,[a,b] KRISTIEN REEKMANS,[a,b] MAXIME DHAINAUT,[c] CAROLINE GUGLIELMETTI,[d] DEBBIE LE BLON,[a,b] DEARBHAILE DOOLEY,[e] ERIK FRANSEN,[f] JASMIJN DAANS,[a,b] LOUCA VERBEECK,[a,b] ALESSANDRA QUARTA,[a,b] NATHALIE DE VOCHT,[a,b] EVI LEMMENS,[e] HERMAN GOOSSENS,[b] ANNEMIE VAN DER LINDEN,[d] VALERIE D. ROOBROUCK,[g] CATHERINE VERFAILLIE,[g] SVEN HENDRIX,[e] MURIEL MOSER,[c] ZWI N. BERNEMAN,[a,b] PETER PONSAERTS[a,b]

Key Words. Interleukin-13 • Mesenchymal stem cells • Allogeneic transplantation • Alternative activation • Macrophages • T cell activation • Graft survival

[a]Laboratory of Experimental Hematology, [b]Vaccine and Infectious Disease Institute, [d]Bio-Imaging Laboratory, [c]Laboratory of Immunobiology, Department of Molecular Biology, Université Libre de Bruxelles, Gosselies, Belgium; [e]Department of Morphology, Biomedical Research Institute, Hasselt University, Diepenbeek, Belgium; [f]StatUa Centre for Statistics, University of Antwerp, Antwerp, Belgium; [g]Stem Cell Institute, Stem Cell Biology and Embryology Unit, KU Leuven, Leuven, Belgium

Correspondence: Peter Ponsaerts, Ph.D., Laboratory of Experimental Hematology, Vaccine and Infectious Disease Institute (Vaxinfectio), University of Antwerp, Campus Drie Eiken (CDE-S6.51), Universiteitsplein 1, 2610 Antwerp (Wilrijk), Belgium. Telephone: 32-3-2652428; e-mail: peter.ponsaerts@uantwerpen.be

Received June 26, 2015; accepted for publication February 12, 2016; first published online in STEM CELLS *EXPRESS* March 17, 2016.

1066-5099/2016/$30.00/0

http://dx.doi.org/10.1002/stem.2360

ABSTRACT

Transplantation of mesenchymal stem cells (MSCs) into injured or diseased tissue—for the in situ delivery of a wide variety of MSC-secreted therapeutic proteins—is an emerging approach for the modulation of the clinical course of several diseases and traumata. From an emergency point-of-view, allogeneic MSCs have numerous advantages over patient-specific autologous MSCs since "off-the-shelf" cell preparations could be readily available for instant therapeutic intervention following acute injury. Although we confirmed the in vitro immunomodulatory capacity of allogeneic MSCs on antigen-presenting cells with standard coculture experiments, allogeneic MSC grafts were irrevocably rejected by the host's immune system upon either intramuscular or intracerebral transplantation. In an attempt to modulate MSC allograft rejection in vivo, we transduced MSCs with an interleukin-13 (IL13)-expressing lentiviral vector. Our data clearly indicate that prolonged survival of IL13-expressing allogeneic MSC grafts in muscle tissue coincided with the induction of an alternatively activated macrophage phenotype in vivo and a reduced number of alloantigen-reactive IFNγ- and/or IL2-producing $CD8^+$ T cells compared to nonmodified allografts. Similarly, intracerebral IL13-expressing MSC allografts also exhibited prolonged survival and induction of an alternatively activated macrophage phenotype, although a peripheral T cell component was absent. In summary, this study demonstrates that both innate and adaptive immune responses are effectively modulated in vivo by locally secreted IL13, ultimately resulting in prolonged MSC allograft survival in both muscle and brain tissue. STEM CELLS *2016;34:1971–1984*

SIGNIFICANCE STATEMENT

Briefly, this manuscript elaborates on the clinical applicability of allogeneic mesenchymal stem cell (MSC) transplantation as a tool for long-term therapeutic protein delivery in vivo, which, despite the presumed immune privileged status of MSCs, is hindered by the host's capacity to induce graft-specific immunity. Here, we established that genetic engineering of allogeneic MSCs with interleukin-13 can modulate graft-directed innate and adaptive host immune responses, evidenced by the in vivo induction of M2a macrophages and the reduced induction of graft-specific $CD8^+$ T cells, with prolonged MSC allograft survival as a result.

INTRODUCTION

Since their initial characterization by Friedenstein et al. [1], mesenchymal stem cells (MSCs) have been the subject of intensive research in the field of regenerative medicine. Although the proposed therapeutic applications of MSCs are numerous, three distinct categories can be identified based on the cells' presumed mode of action: direct cell replacement [2–6], immunomodulation [7–14], and trophic stimulation of endogenous regeneration by (genetically modified) MSC grafts [14–19]. MSCs can thus be adopted as versatile cell-based delivery vehicles for therapeutic proteins in a wide range of conditions, extending from hematological [13, 20, 21]

and cardiovascular [4, 22] disorders to autoimmune [5, 23] and central nervous system (CNS) [7, 14–16] pathologies. Although both autologous and allogeneic MSCs have been translated into the clinic [12, 13, 24, 25], the prospect of using universal donor MSCs provides the most attractive alternative, as "off-the-shelf" cell preparations could be readily available for instant therapeutic intervention following acute injury. In addition, autologous patient-derived cells may be compromised due to age or disease [5, 26]. Moreover, the use of allogeneic cells enables the careful selection of (genetically engineered) cell populations displaying maximal effectiveness (i.e., regenerative capacity [27]) and minimal adverse effects (i.e., tumorigenicity [17]).

Even though it is widely accepted that MSCs display a range of immunosuppressive properties in vitro [28–30], the in vivo immune privileged status of MSCs remains a matter of controversy [25]. Over the years, scientists have often regarded the long-term clinical benefit of allogeneic or xenogeneic MSC transplantation as evidence of their immune privileged character, an assumption only occasionally supported by experiments exploring the fate or in vivo immunogenicity of the transplanted cells [2–5, 10, 11, 13, 31]. In order to safely and effectively apply MSC therapy in disease, it is however of the utmost importance to establish a clear relationship between the in vivo fate of grafted MSCs and the observed clinical response [32]. Biodistribution of the grafted MSCs is a first factor to consider following in vivo cell administration. After intravenous (IV) administration of MSCs, only a very small percentage of the infused MSCs (usually $< 1\%$) reach the target tissue due to cell retention in the lungs, liver, and spleen [22, 33–35]. Following their entrapment, embolized MSCs release paracrine factors such as tumor necrosis factor-stimulated gene 6 (TSG-6) which induce a general state of immune hyporesponsiveness, resulting in an improved therapeutic outcome in inflammation-associated diseases [22, 36, 37]. However, injuries at more distant locations in the body do not always respond equally well to this approach [35, 38]. In these instances, direct cell grafting into (injured) tissue might have a more pronounced therapeutic benefit. MSCs are known producers of immunomodulatory (e.g., interleukin-6 (IL6), IL10, prostaglandin E2 (PGE_2), and indoleamine 2,3-dioxygenase (IDO) [9]), neurotrophic (e.g., brain-derived neurotrophic factor (BDNF) and nerve growth factor (NGF) [39]), and angiogenic factors (e.g., vascular endothelial growth factor (VEGF) [40]). For this reason, their therapeutic application following neurotrauma (e.g., stroke and traumatic brain/spinal cord injury [39, 41]) and peripheral vascular disease (i.e., ischemia [40]) can readily be appreciated upon intracerebral (IC) or intramuscular (IM) application, respectively. Immunogenicity is another important determinant of cell fate, especially when allogeneic cells are used. It is imperative to investigate whether allogeneic MSCs have the capacity to survive immunologically for a sufficiently long period of time in order to be of clinical relevance. Eliopoulos et al. [42] were among the first to investigate this matter, describing the presence of alloantigen-reactive $CD8^+$ T cells, natural killer (NK) T cells, and NK cells following MSC transplantation in major histocompatibility complex (MHC)-mismatched mice. They also found evidence of immunological memory against allografts as repeated MSC transplantations resulted in accelerated graft rejection. Several reports, including our own work, have validated Eliopoulos' findings, additionally describing robust myeloid cell infiltration of allografts and the induction of allograft-specific antibody responses [33, 43–45]. In the first part of this study, we further elaborated on the immunosuppressive capacities of MSCs in vitro versus in vivo in an effort to unify conflicting literature reports. Although we confirmed the immunomodulatory capacity of allogeneic MSCs on dendritic cells (DCs) using standard in vitro coculture experiments, MSC grafts were rapidly rejected upon IV, IM, or IC transplantation into allogeneic hosts. Furthermore, we found that MSC-mediated suppression is cell contact-dependent, as MSC-primed DCs became highly immunostimulatory upon MSC withdrawal.

IL13 is a pleiotropic cytokine closely related to IL4 both in structure and in function [46]. These canonical cytokines play overlapping as well as distinct roles during type 2 immunity, and both factors have been found to contribute to the etiology of allergic reactions. Despite their similar biological activities, IL4 signaling in T helper cells promotes Th2 differentiation, whereas T cells are generally unresponsive to IL13 due to the absence of IL13Rα1 expression on their surface [47]. In the second part of this study, we genetically modified allogeneic MSCs with the murine IL13-encoding gene as a potential strategy to modulate allograft-specific immunity and extend in vivo cell graft survival following IM and/or IC transplantation. We focused specifically on IL13 as no evidence has been found to date that this cytokine promotes T cell stimulation or proliferation upon direct exposure, in contrast to IL4 [48], hence limiting the risk of inducing allergic side effects. In this study, we were able to demonstrate that local secretion of IL13 induced the M2a alternative activation state in graft-infiltrating macrophages (and microglia) and limited the induction of alloreactive $CD8^+$ T cells. As a result, IL13-mediated modulation resulted in a prolongation of allogeneic cell graft survival in both muscle and brain tissue of immune competent mice.

Materials and Methods

Mice

C57BL/6, FVB, and BALB/c mice were purchased from Charles River (Wilmington, MA, http://www.criver.com). Albino C57BL/6, C57BL/6 $IL6^{-/-}$, and FVB ROSA26-L-S-L-Luciferase mice were purchased from Jackson Laboratories (Bar Harbor, ME, http://www.jax.org). All mice, including (C57BL/6 $\times$ FVB) F_1 hybrids, were bred in the animal facility of the University of Antwerp. All experimental procedures were approved by the ethical committee for animal experiments at the University of Antwerp (approval nos. 2011/13 and 2012/39).

Isolation, Genetic Engineering, and Characterization of MSC Cultures

FVB, ROSA26-L-S-L-Luciferase, and BALB/c mouse bone marrow-derived MSC cultures were isolated and cultured as previously described by Bergwerf et al. [49]. The following lentiviral vectors (LVs) were used for MSC transduction: pCHMWS-eGFP-T2A-fLuc [50], pCHMWS-eGFP-IRES-Pac [49], and pCHMWS-mIL13-IRES-Pac. LV production was outsourced to the Leuven viral vector core (Molmed, KULeuven, Belgium) [51, 52]. Following LV transduction, Pac-expressing MSCs were selected with puromycin (10 μg/mL; InvivoGen, San Diego, CA, http://www.invivogen.com). For cells transduced with the pCHMWS-eGFP-T2A-fLuc LV,

a clonal line was obtained by limiting dilution and selected based on enhanced green fluorescent protein (eGFP) expression and firefly luciferase activity [49]. Expression of eGFP, luciferase, and/or IL13 was evaluated by, respectively, flow cytometry using GelRed (Biotium, Hayward, CA, https://biotium.com) for dead cell exclusion (Epics XL-MCL; Beckman Coulter, Fullerton, CA, http://www.beckmancoulter.com), in vitro luminometry (Bright-Glo; Promega, Madison, WI, http://www.promega.com), and murine IL13 ELISA (Peprotech, Rocky Hill, NJ, http://www.peprotech.com). A detailed immunophenotypic analysis, including the expression of MSC lineage-specific markers (CD29, CD44, CD106, and Sca-1) as well as endothelial and hematopoietic (CD31 and CD45, respectively) markers, of all MSC lines used in this study is provided in Supporting Information Figure S1.

Cell Implantation Experiments

All surgical interventions were performed according to previously established procedures [45, 53]. For IC cell injection, mice were anesthetized with a ketamine (80 mg/kg, Pfizer, New York, NY, http://www.pfizer.com) + xylazine (16 mg/kg, Bayer, Leverkusen, Germany, http://www.bayer.com) mixture in 0.9% NaCl (Baxter, Deerfield, IL, http://www.baxter.com) and placed in a stereotactic frame (Stoelting, Wood Dale, IL, http://www.stoeltingco.com). 7.5×10^4 MSCs (in 2 μL phosphate buffered saline (PBS)) were reproducibly targeted to the right hemisphere, 2.25 mm dextra, and 3.00 mm ventral from bregma. For IM cell injection, mice were anesthetized in an induction chamber using an isoflurane (2.5%) (Forene, AbbottAbbott Park, IL, http://www.abbott.com) + N_2O (1 L/min) + O_2 (0.5 L/min) gas mixture, and 5×10^5 MSCs or 3×10^5 DCs (in 100 μL PBS) were injected in the right (or left) pelvic limb muscle. For IV cell injection, mice were anesthetized using isoflurane (2.5% + 1 L/minute N_2O + 0.5 L/minute O_2) and 7.5×10^4 MSCs (in 100 μL PBS) were administered via the tail vein.

In Vivo Bioluminescence Imaging

At different time points between day 1 and day 17 after cell implantation, (albino) C57BL/6 mice were analyzed by real-time in vivo bioluminescence imaging (BLI) to determine the presence of viable cell implants and their biodistribution. Mice were anesthetized using a mixture of isoflurane (Forene, Abbott; 2.5% induction and 2% maintenance) and oxygen. One minute after IV D-luciferin administration (150 mg/kg in PBS; Promega), mice were imaged using a real-time Photon Imager (Biospace Lab, Nesles-la-Vallée, France, http://www.biospacelab.com) or an IVIS Spectrum imaging system (Caliper Life Sciences, Hopkinton, MA, http://caliperls.com was recently acquired by PerkinElmer, Waltham, MA, http://www.perkinelmer.com). Data were acquired and analyzed with M3Vision (Biospace Lab) or Living Image (Caliper) software.

Functional Analysis of Splenic DCs

Spleens were digested with collagenase type III (Worthington Biochemicals, Lakewood, NJ, www.worthington-biochem.com), further dissociated in Ca^{2+}-free medium, and separated into high and low density fractions on a Nycodenz gradient (Nycomed, Asker, Norway, http://www.nycomed.com was recently acquired by Takeda Pharmaceuticals, Zürich, Switzerland, http://www.tpi.takeda.com). Low density cells were retrieved from the interphase, and DCs were enriched by magnetic separation with CD11c MicroBeads (Miltenyi Biotec, Bergisch Gladbach, Germany, http://www.miltenyibiotec.com). For all isolations, > 90% DC purity was achieved, as determined by antibody staining with phycoerythrin-labeled anti-mouse CD11c (12-0114; eBioscience, San Diego, CA, http://www.ebioscience.com) and measurement with an Epics XL-MCL analytical flow cytometer (Beckman Coulter). Following isolation, DCs were either cultured alone or brought in coculture with FVB MSCs or FVB MSCs-IL13 (ratio 2:1 or 5:1 for ELISA or DC vaccination experiments, respectively). For subsequent ELISA, 1 μg/mL lipopolysaccharide (LPS; InvivoGen) + 500 U/mL interferon-γ (IFNγ; ImmunoTools, Friesoythe, Germany, http://www.immunotools.de) was added to the cell cultures, and supernatants were harvested 24 hours later. MSC-DC supernatants were tested for the presence of various cytokines using the following murine ELISAs: tumor necrosis factor alpha (TNFα) (BioLegend, San Diego, CA, http://www.biolegend.com), IL4 (Peprotech), IL6 (BioLegend), IL10 (eBioscience), and IL13 (Peprotech). For DC vaccination experiments, cell cultures were supplemented with 20 ng/mL granulocyte-macrophage colony-stimulating factor (GM-CSF) (ImmunoTools). Following 48 hours of coculture, DCs were harvested and resuspended at a concentration of 3×10^5 cells per 100 μL PBS for IM vaccination in C57BL/6 mice.

Detection of Alloantigen-Specific T Cell Responses

Two weeks after MSC grafting or DC vaccination, spleens were surgically removed and dissociated over a 70 μm nylon mesh. After density-based centrifugation (Ficoll-Paque Plus; GE Healthcare, Little Chalfont, United Kingdom, http://www3.gehealthcare.com), T cells were enriched by magnetic separation with mouse CD4, CD8a, or CD90.2 MicroBeads (Miltenyi Biotec). Isolated T cell populations were seeded in 96-well round-bottom or ELISpot plates under the following conditions: (a) no stimulation, (b) general stimulation: phorbol 12-myristate 13-acetate (PMA) (50 ng/mL, Sigma-Aldrich, Saint Louis, MO, https://www.sigmaaldrich.com) + ionomycin (500 ng/mL, Sigma-Aldrich), and (c) antigen-specific stimulation: MSCs (ratio 10:1) or DCs (ratio 10:1).

For subsequent flow cytometric analysis, $CD90.2^+$ cells were stimulated for 4 hours at 37 °C in the presence of monensin (0.67 μL/mL GolgiStop; BD Biosciences, San Diego, CA, http://www.bdbiosciences.com), and intracellular cytokine staining was performed on the cells using the antibodies listed in Supporting Information Table 1. T cell cytokine production was measured on a FACSAria II cell sorter and analyzed using the FACSDiva software (both BD Biosciences). A detailed visualization of the gating strategy used to determine the percentages of $CD4^+$ and $CD8^+$ T cells producing the cytokines IL2, IFNγ, IL4, and IL17 is provided in Supporting Information Figure S2. For subsequent ELISpot analysis, $CD8^+$ T cells were stimulated for 16 hours at 37 °C and used in a murine IFNγ ELISpot assay (Diaclone, Besançon, France, http://www.diaclone.com). For IFNγ ELISA, $CD4^+$ and $CD8^+$ T cells were stimulated for 16 hours at 37 °C. Supernatants were collected and analyzed with the murine IFNγ ELI-pair (Diaclone) according to the manufacturer's protocol.

Detection of Allograft-Specific Antibody Responses

FVB MSCs were preincubated with whole serum (1:6 dilution) derived from control, FVB MSC-, or FVB MSC-IL13-grafted mice and stained using labeled isotype-specific secondary antibodies, listed in Supporting Information Table 1. Flow cytometric analysis was performed on an Epics XL-MCL analytical flow cytometer (Beckman Coulter) or on a FACSAria II cell sorter (BD Biosciences),

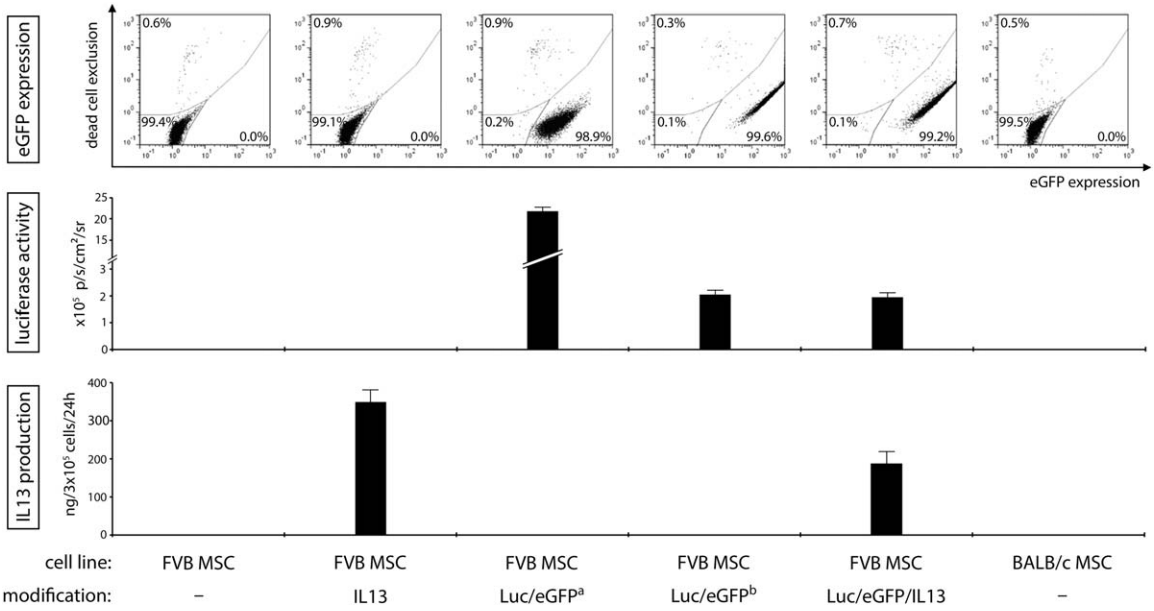

Figure 1. Characterization of the genetically engineered MSCs used in this study. FVB mouse-derived MSCs (column 1: FVB MSC) were transduced using the pCHMWS-mIL13-IRES-Pac LV (column 2: FVB MSC-IL13) or the pCHMWS-eGFP-T2A-fLuc LV (column 3: FVB MSC-Luc/eGFP[a]). A previously established ROSA26-L-S-L-Luciferase mouse-derived eGFP-expressing MSC line [49] (column 4: FVB MSC-Luc/eGFP[b]) was additionally transduced with the pCHMWS-mIL13-IRES-Pac LV (column 5: FVB MSC-Luc/eGFP/IL13). BALB/c mouse-derived MSCs (column 6: BALB/c MSC) were used without further modification. Top panel: Percentage of $eGFP^+$ (lower right gate) and $eGFP^-$ (lower left gate) cell populations, following dead cell exclusion with GelRed (upper gate). Representative dot plots are shown from three independent experiments. Middle panel: In vitro bioluminescence imaging of 1×10^5 cells, expressed as photons per second per square centimeter per steradian $\pm$ SD ($n = 3$). Lower panel: IL13 production by 3×10^5 MSCs during 24 hours of culture. Data are presented as mean $\pm$ SD ($n = 3$). Abbreviations: eGFP, enhanced green fluorescent protein; IL, interleukin; Luc, firefly luciferase; LV, lentiviral vector; MSC, mesenchymal stem cell.

and data were analyzed using FlowJo (FlowJo LLC, Ashland, OR, http://www.flowjo.com).

Histological Analysis

Mice were deeply anesthetized with an intraperitoneal injection of 60 mg/kg pentobarbital (Nembutal; Ceva Santé Animale, Libourne, France, http://www.ceva.com), transcardially perfused with 0.9% NaCl, and perfused-fixed with 4% paraformaldehyde. Whole brain/pelvic limb muscles were surgically removed and postfixed in 4% paraformaldehyde. Fixed tissues were freeze-protected with a sucrose gradient, snap-frozen in liquid nitrogen, and 10 μm thick cryosections were made. Immunofluorescent staining was performed according to previously optimized procedures [53, 54] using the antibodies listed in Supporting Information Table 1. Stained slides were mounted with Prolong Gold antifade reagent (Life Technologies, Rockville, MD, http://www.lifetech.com), and images were acquired using an Olympus BX51 fluorescence microscope equipped with an Olympus DP71 digital camera. Olympus cellSens Dimension software was used for image acquisition and processing (Olympus, Tokyo, Japan, http://www.olympus-global.com).

In Vivo LV Injection Experiments

The following LVs were used for in vivo administration: pCHMWS-mIL13-IRES-Pac and pCHMWS-BFP-IRES-Pac [55]. All surgical interventions were performed according to previously established procedures [56]. Briefly, C57BL/6 mice (8 weeks of age) were anesthetized with a ketamine (75 mg/kg; Eurovet, Bladel, The Netherlands (no website found) was recently acquired by Dechra Pharmaceuticals, Northwich, United Kingdom, http://www.dechra.com) + medetomidine (1 mg/kg; Pfizer) mixture in 0.9% NaCl (Baxter) and placed in a stereotactic frame (Stoelting). 2 μL of LV concentrate (1.5×10^7–3×10^7 pg/mL p24) was reproducibly targeted to the splenium of the corpus callosum at 1.6 mm posterior and 0.3 mm dextra from bregma and 1.1 mm ventral from the dura. Anesthesia was reversed with an intraperitoneal injection of atipamezole (0.5 mg/kg; Pfizer).

Induction of Cuprizone-Associated Inflammatory CNS Lesions

At the age of 8 weeks, mice with or without prior LV injection received standard rodent chow mixed with 0.2% w/w cuprizone (CPZ; Sigma-Aldrich) for a period of 4 weeks in order to induce neuroinflammation and CNS demyelination, as previously described [56–59].

Statistical Analysis

All numeric outcome variables were tested for normality and, if needed, log-transformed to obtain an approximately normal distribution. The following statistical tests were used: (a) one-way ANOVA for TNFα/IL6 ELISA data and for the flow cytometric detection of antibody responses, (b) generalized linear mixed modeling for the flow cytometric detection of T cell cytokine production, (c) two-way ANOVA or one-way ANOVA with subsequent independent t-test for IFNγ ELISpot data, (d) linear mixed modeling for IFNγ ELISA data and in vivo bioluminescence, and (e) Mantel-Cox testing for in vivo cell survival analysis. When required, post hoc analyses were performed and resulting *p* values were adjusted using a Tukey correction for multiple testing. The Mantel-Cox test was performed using GraphPad Prism

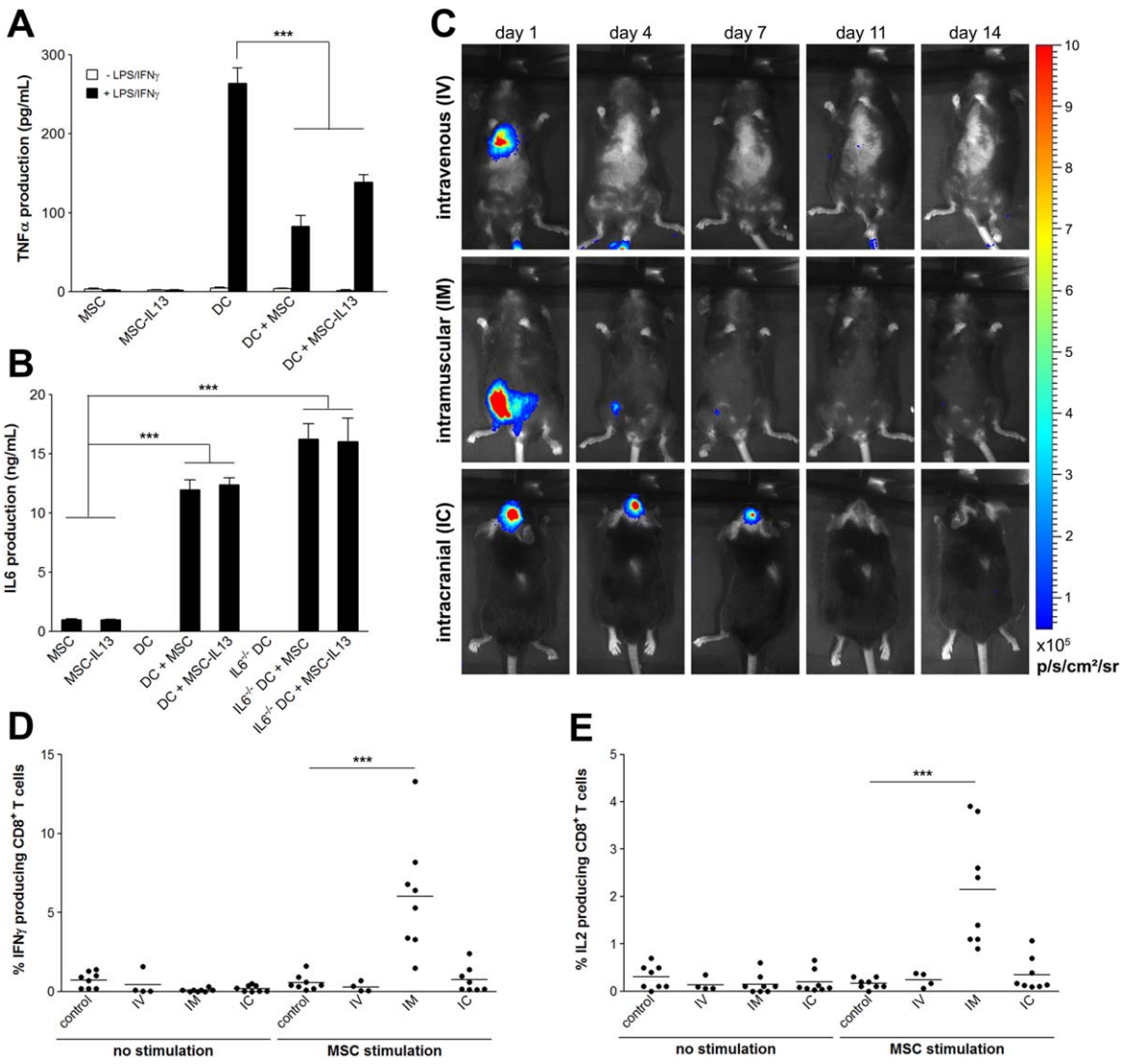

Figure 2. Immunogenicity and immunomodulatory properties of allogeneic MSCs: in vitro versus in vivo. **(A)**: TNFα production by C57BL/6-derived splenic DCs cocultured with FVB MSCs or FVB MSCs-IL13, with or without LPS/IFNγ stimulation. Representative data from one of three independent stimulation experiments are shown as mean ± SD, with all conditions tested in quadruplicate. **(B)**: IL6 production by LPS/IFNγ-stimulated FVB MSCs or FVB MSCs-IL13 cocultured with wild-type or $IL6^{-/-}$ C57BL/6-derived splenic DCs. Data are presented as mean ± SD, with all conditions tested in sextuplicate. **(C)**: In vivo bioluminescence imaging of FVB MSCs-Luc/eGFP[a] in C57BL/6 mice following IV ($n = 3$), IM ($n = 2$), or IC ($n = 3$) cell administration. Representative time course images are shown. The most intense bioluminescence signal is shown in red, the weakest in blue. Light intensity is presented as the average number of photons per second per square centimeter per steradian. **(D, E)**: Allograft-specific $CD8^+$ T cell responses. T cells from naive C57BL/6 mice (control, $n = 8$) and from C57BL/6 mice given an IV ($n = 4$), IM ($n = 8$), or IC ($n = 8$) FVB MSC transplant were analyzed by flow cytometry, with or without prior stimulation with FVB MSCs. Data are presented as % $CD8^+$ T cells positive for the cytokines IFNγ or IL2. ***, $p < .001$. Abbreviations: DC, dendritic cell; IC, intracerebral; IFNγ, interferon-γ; IL, interleukin; IM, intramuscular; IV, intravenous; MSC, mesenchymal stem cell; LPS, lipopolysaccharide; TNFα, tumor necrosis factor alpha.

software version 5. All remaining statistical analyses were performed using the statistical package R version 3.1.2. p values $< .05$ were considered statistically significant: *, $p < .05$; **, $p < .01$; ***, $p < .001$; n.s., not significant.

Results

Allogeneic MSCs Are Subject to Immune Recognition In Vivo, Despite Their Immunomodulatory Properties In Vitro

In the first part of this study, we assessed the immunological properties of allogeneic MSCs in vitro versus in vivo. Coculture experiments of FVB mouse-derived MSCs (Fig. 1: FVB MSC) with LPS/IFNγ-activated C57BL/6 splenic DCs confirmed the in vitro immunomodulatory capacity of MSCs, illustrated by a reduction in TNFα secretion by DCs (Fig. 2A) and an elevation in IL6 production by MSCs (Fig. 2B). In contrast, grafted luciferase/eGFP-expressing FVB MSCs (Fig. 1: FVB MSC-Luc/eGFP[a]) rapidly became undetectable by in vivo BLI following IV, IM, and IC implantation in C57BL/6 mice (Fig. 2C). IV administration of FVB MSCs-Luc/eGFP[a] resulted in cell entrapment in the lungs followed by rapid loss of the BLI signal. IM and IC MSC allografts, on the other hand, could be detected—with decreasing signal intensity—up to 1 week postinjection at their original site of implantation. Additionally, we investigated whether FVB

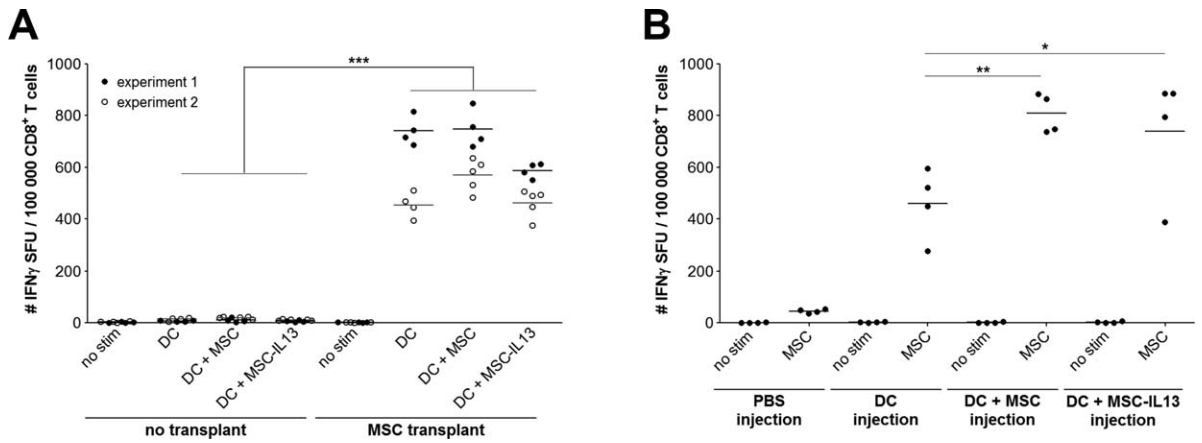

Figure 3. MSC-primed DCs become highly immunostimulatory upon withdrawal of MSC contact. **(A)**: Effect of MSC priming on the induction of secondary T cell responses in vitro. In vitro unprimed, FVB MSC-primed, and FVB MSC-IL13-primed DCs from (C57BL/6 × FVB) F_1 mice were used as stimulator cells (DC, DC+MSC, and DC+MSC-IL13, respectively) in an IFNγ ELISpot assay with $CD8^+$ T cells from naive (no transplant) or IM FVB MSC-transplanted C57BL/6 mice. No DCs were added to the control condition (no stim). Two independent experiments were performed in which every condition was tested at least in quadruplicate. Data are presented as the number of IFNγ SFU per 10^5 responder $CD8^+$ T cells. **(B)**: Effect of MSC priming on the induction of primary T cell responses in vivo. In vitro unprimed, FVB MSC-primed, and FVB MSC-IL13-primed DCs from (C57BL/6 × FVB) F_1 mice were used for IM vaccination in C57BL/6 mice (DC injection, DC+MSC injection, and DC+MSC-IL13 injection, respectively). Subsequently, $CD8^+$ T cells were isolated from naive (PBS injection) or vaccinated C57BL/6 mice ($n = 4$ per group) and used in an IFNγ ELISpot assay with FVB MSCs as stimulator cells. Data are presented as the number of IFNγ SFU per 10^5 responder $CD8^+$ T cells. ***, $p < .001$. Abbreviations: DC, dendritic cell; IL, interleukin; IFNγ, interferon-γ; MSC, mesenchymal stem cell; PBS, phosphate buffered saline; SFU, spot-forming unit.

allograft-specific T cell responses were induced upon MSC infusion via these different administration routes (Fig. 2D, 2E). In agreement with and further extending our preceding observations [45], substantial numbers of $IFN\gamma^+$ and $IL2^+$ alloantigen-reactive $CD8^+$ T cells were present in IM grafted mice. Interestingly, $IFN\gamma^+$ and $IL2^+$ alloantigen-reactive $CD8^+$ T cells were not found following IV or IC transplantation. Allograft-specific $CD4^+$ T cell responses (Th1/Th2) and Th17/Tc17 responses were not detected in any of the tested conditions (Supporting Information Fig. S3). The induction of alloantigen-reactive $CD8^+$ T cells following IM administration of MSCs was additionally confirmed by means of IFNγ ELISpot and ELISA (Supporting Information Fig. S4).

In Vitro MSC-Primed DCs Become Highly Immunostimulatory, Both In Vitro and In Vivo, Upon Withdrawal of MSC Contact

In the previous paragraph, we described seemingly contradictory effects of allogeneic MSCs in vitro versus in vivo: even though they had an immunomodulatory effect on DC function under in vitro conditions (Fig. 2A), a manifest induction of MSC-specific T cells was observed upon their IM implantation in an allogeneic host (Fig. 2D, 2E). In order to further investigate this discrepancy, we examined whether MSC-primed DCs displayed a reduced T cell stimulatory capacity in vitro upon withdrawal of MSC contact. Splenic DCs were isolated from (C57BL/6 × FVB) F_1 mice, cocultured in vitro with FVB MSCs, and used to restimulate $CD8^+$ T cells isolated from naive or FVB MSC-grafted C57BL/6 mice in an IFNγ ELISpot assay (Fig. 3A). Using this experimental setup, we found no reduction in the T cell stimulatory capacity of MSC-primed DCs, compared to unprimed DCs, upon withdrawal of MSC contact. In a subsequent experiment, we studied the in vivo T cell induction capacity of MSC-primed DCs. Splenic DCs from (C57BL/6 × FVB) F_1 mice, either unprimed or primed with FVB MSCs, were injected intramuscularly into C57BL/6 mice. An IFNγ ELISpot assay using $CD8^+$ T cells from these injected mice revealed the efficient induction of FVB alloantigen-specific $CD8^+$ T cell responses following DC vaccination, regardless of prior MSC priming (Fig. 3B). Surprisingly, MSC-primed DCs induced even more alloreactive T cells in vivo than unprimed DCs. Upon withdrawal of MSC contact, in vitro MSC-primed DCs thus became highly immunostimulatory, supporting the notion that MSC-mediated modulation is cell contact-dependent [29].

Genetic Engineering of MSC Allografts with IL13 Reduces the Induction of Peripheral Allograft-Specific T Cell Responses

Since allogeneic MSCs were found to elicit a significant T cell response upon IM transplantation, we investigated whether the neoexpression of IL13 by allogeneic MSCs could (partially) counteract this induction of alloreactive T cells following IM MSC transplantation. To this end, we evaluated the occurrence of allograft-specific T cell responses in C57BL/6 mice 2 weeks after IM transplantation of control FVB MSCs or IL13-producing FVB MSCs (Fig. 1: FVB MSC-IL13). Both transplant groups displayed significant allograft-specific $CD8^+$ T cell responses, although mice with IL13-producing allografts were characterized by significantly fewer $IFN\gamma^+$ and $IL2^+$ $CD8^+$ T cells (Fig. 4A, 4B). Similarly to the aforementioned results, allograft-specific $CD4^+$ T cell responses, as well as Th17/Tc17 responses, were not detected in any of the experimental groups (Supporting Information Fig. S5). As T cells lack a functional IL13 receptor on their cell surface [47], it is highly unlikely that IL13 exerts its effect on T cell functionality at the level of the T cells themselves. Indeed, when T cells isolated from FVB MSC-grafted mice were restimulated in vitro with either FVB MSCs or FVB MSCs-IL13, no difference in IFNγ production by isolated $CD8^+$ T cells was seen (Fig. 4C). Conditions in which MSCs had been precultivated in the well for 24 hours prior to coculture were included to ensure a sufficiently high IL13 concentration throughout MSC-T cell interaction. Although IFNγ

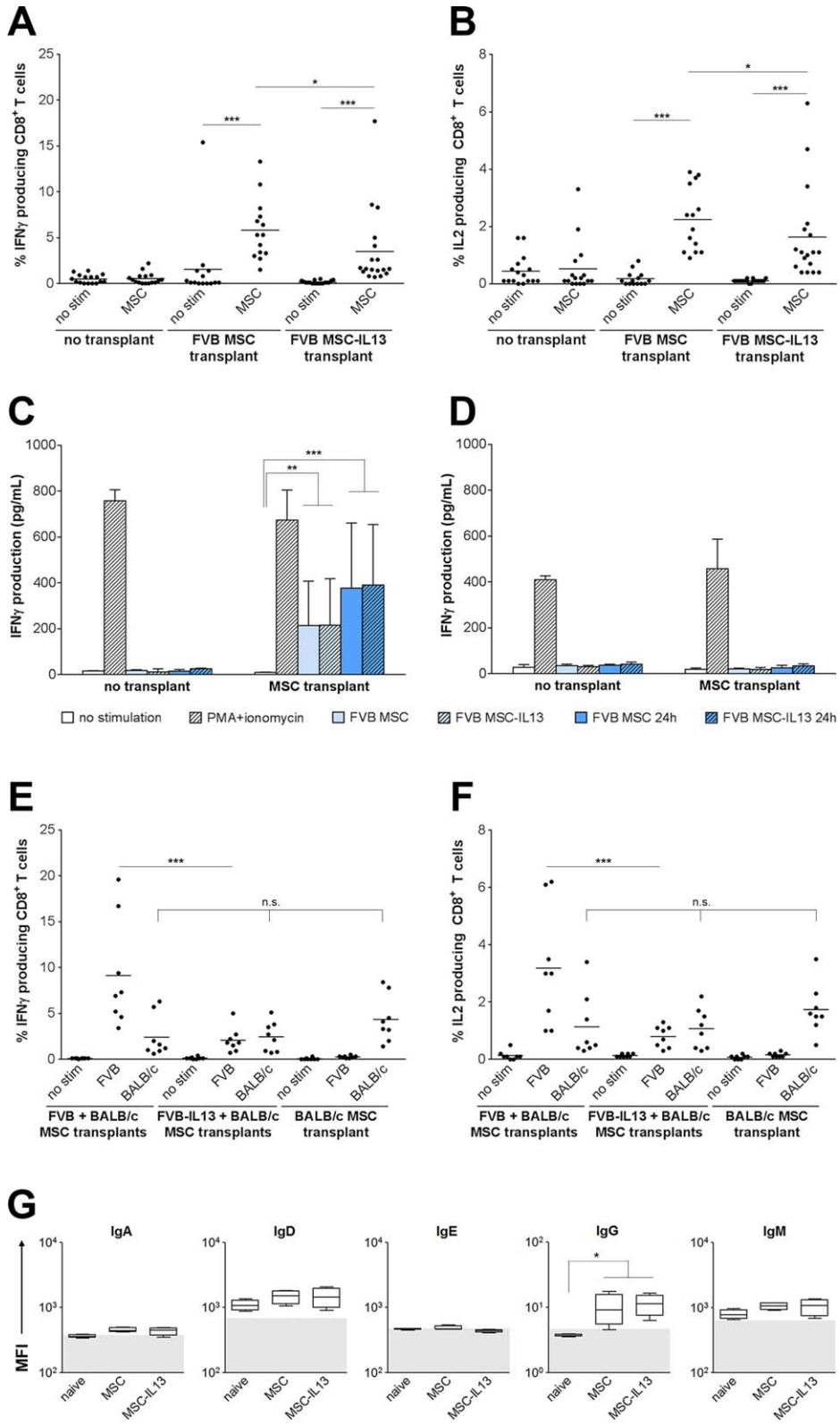

Figure 4. Grafting of IL13-producing allogeneic MSCs results in a reduced induction of alloreactive T cells without affecting allograft-specific humoral responses. **(A, B)**: Allograft-specific $CD8^+$ T cell responses. T cells from naive (no transplant, $n = 16$), FVB MSC-transplanted ($n = 14$), or FVB MSC-IL13-transplanted ($n = 18$) C57BL/6 mice were analyzed by flow cytometry, with or without prior FVB MSC stimulation. Data are presented as % $CD8^+$ T cells positive for IFNγ or IL2. **(C, D)**: Effect of IL13 on activated T cells. T cells from naive (no transplant, $n = 1$) or FVB MSC-transplanted C57BL/6 mice ($n = 3$) were restimulated under the following conditions: no stimulation, PMA + ionomycin stimulation, and FVB MSC(±IL13) stimulation. IFNγ production by T cells was quantified by ELISA. Data are presented as mean ± SD, with each condition tested in triplicate for each mouse. **(E, F)**: $CD8^+$ T cell responses against FVB and BALB/c MSC allografts. T cells from MSC transplanted mice ($n = 8$ per group) were analyzed by flow cytometry, with or without prior stimulation with FVB or BALB/c MSCs. Data are presented as % $CD8^+$ T cells positive for IFNγ or IL2. **(G)**: Allograft-specific antibody responses. FVB MSCs were incubated with serum samples from naive C57BL/6 mice or from mice challenged with IM FVB MSC(±IL13) allografts ($n = 4$ per group), stained with labeled isotype-specific secondary antibodies and analyzed by flow cytometry. Background fluorescence (MSCs + secondary antibody alone) is demarcated by the gray area. Data are expressed as MFI. n.s., not significant; *, $p < .05$; **, $p < .01$; ***, $p < .001$. Abbreviations: IFNγ, interferon-γ; IL, interleukin; MFI, mean fluorescence intensity; MSC, mesenchymal stem cell; PMA, phorbol 12-myristate 13-acetate.

production by $CD8^+$ T cells was elevated in the latter, primed T cells were not influenced by the presence of IL13 in the supernatant. In agreement with our other results, IFNγ production by $CD4^+$ T cells was not detected (Fig. 4D).

Short-Term In Vitro IL13-Priming of DCs Cannot Recapitulate Complex In Vivo Interactions Between Allogeneic MSCs, IL13, Antigen-Presenting Cells, and T Cells

As IL13 has been shown to effectively reduce the induction of peripheral T cell responses without acting directly on activated T cells, we hypothesized that the cytokine must exert its effect at the level of antigen-presenting cells (APCs). Like nonengineered MSCs, IL13-expressing MSCs reduced TNFα production by DCs (Fig. 2A) and are induced to produce IL6 upon DC coculture (Fig. 2B). Unexpectedly, in vitro IL13-primed C57BL/6×FVB DCs did not display a reduced T cell stimulatory capacity in vitro (Fig. 3A) or in vivo (Fig. 3B) in comparison to nonengineered MSCs. Clearly, the intricate mechanism(s) by which IL13 modulates allospecific T cell responses in vivo are far too complex to be simulated in vitro.

IL13-Mediated T Cell Modulation is Restricted to Alloantigens Present at the Site of IL13 Secretion and Does Not Coincide with Changes in Allograft-Specific Antibody Response

Next, we questioned whether IL13 only modulated the alloimmune response directed toward the IL13-expressing FVB MSC allograft or whether MSC-derived IL13 could additionally modulate alloimmune responses directed toward a distant, third-party allograft. To investigate this, C57BL/6 mice received a BALB/c MSC allograft (Fig. 1: BALB/c MSC) in the left hind limb and, if applicable, an additional FVB MSC or FVB MSC-IL13 allograft in the right hind limb. Using this setup, we validated the finding that the percentage of FVB alloantigen-specific IFNγ- and IL2-producing $CD8^+$ T cells was significantly reduced in mice with an IL13-producing MSC graft compared to mice with a control MSC graft (Fig. 4E, 4F and Supporting Information Fig. S6). Interestingly, the relative number of BALB/c alloantigen-specific IFNγ- and IL2-producing $CD8^+$ T cells was comparable in all BALB/c MSC-grafted mice, regardless of the presence of an additional FVB MSC(±IL13) graft. This thus suggests that the observed IL13-mediated immunomodulation is restricted to FVB MSC antigens, that is, alloantigens present at the site of IL13 secretion and does not suppress immune responses against distant third-party allografts. Finally, we investigated the potential of MSC-derived IL13 to modulate allograft-specific antibody responses. Two weeks after IM transplantation of FVB MSCs or FVB MSCs-IL13, whole serum was collected from transplanted or naive C57BL/6 mice and evaluated for the presence of allograft-specific antibodies (Fig. 4G). FVB MSC-specific antibodies of the IgG isotype—but not of the IgA, IgD, IgE, and IgM isotypes—could readily be detected in all transplanted mice. No modulatory effect of IL13 on the antibody response was observed as comparable levels of graft-specific IgG antibodies were found in mice grafted with nonengineered or IL13-expressing MSCs.

Transplantation of IL13-Producing MSCs Induces an Alternatively Activated Phenotype in Graft-Infiltrating Macrophages

As IL13 is a key cytokine in the promotion of alternative macrophage activation [46], we examined whether IL13-producing MSC allografts were able to induce an alternatively activated phenotype in graft-infiltrating macrophages (and microglia in the case of IC grafts [55]). Histological analyses of FVB MSC-Luc/eGFP^b grafts (Fig. 1: FVB MSC-Luc/eGFP^b) and FVB MSC-Luc/eGFP/IL13 grafts (Fig. 1: FVB MSC-Luc/eGFP/IL13) were performed at 5 (IM grafts) or 7 (IC grafts) days after implantation in C57BL/6 mice. At given time points, all eGFP-expressing MSC grafts—or remnants thereof in case of IC FVB MSC-Luc/eGFP^b transplantation—could readily be detected (Fig. 5, first row). MSC allografts displayed a substantial infiltration of activated macrophages (and microglia) under all experimental conditions, as demonstrated by the presence of $Iba1^+$ and $F4/80^+$ myeloid cells within and surrounding MSC grafts (Fig. 5, second-fourth rows). The classic activation marker MHCII was expressed by graft-infiltrating $F4/80^+$ macrophages (and microglia) in all tested conditions (Fig. 5, third and fifth rows). In contrast, the expression of Arg1, a marker of alternative M2a activation [46, 60], was exclusive to $F4/80^+$ macrophages (and microglia) infiltrating IL13-producing grafts (Fig. 5, fourth and fifth rows). Similarly, the expression of Ym1 and FIZZ1, two additional M2a markers [46], was restricted to myeloid cells associated with IL13-producing MSC grafts (Fig. 5, sixth row). Graft-infiltrating $CD3^+$ and $CD8^+$ T cells were observed under all experimental conditions (Fig. 5, seventh and eighth rows).

IL13 Alone is Sufficient to Induce In Vivo M2a Macrophage/Microglia Polarization

In a subsequent experiment, we investigated whether the in vivo M2a polarization of macrophages and microglia observed following grafting of IL13-expressing MSCs is induced by the single action of IL13 or by a combined effect of MSCs and IL13. For this, we examined whether expression of IL13 in the splenium of the corpus callosum could induce alternative M2a polarization of microglia and macrophages following CPZ administration, a well-established mouse model of neuroinflammation [56, 61]. As shown in Figure 6, CPZ administration leads to severe accumulation of $F4/80^+$ microglia/macrophages in the splenium of non-injected control mice, blue fluorescent protein (BFP)-expressing control LV-injected mice and IL13-expressing LV-injected mice. In vivo administration of IL13-expressing LV additionally induced Arg1 expression in CPZ lesion-associated microglia/macrophages, indicating that IL13 alone can effectively induce M2a microglia/macrophage polarization.

IL13 Prolongs MSC Allograft Survival Upon IM and IC Administration

In a final experiment, we investigated whether the production of IL13 by MSCs could alter the course of MSC allograft rejection. To this end, the in vivo survival of FVB MSC-Luc/eGFP^b and FVB MSC-Luc/eGFP/IL13 allografts was evaluated noninvasively by quantitative in vivo BLI following IM (Fig. 7A–7C) and IC (Fig. 7D–7F) implantation in albino C57BL/6 mice. Allograft survival, defined as the time point beyond which the bioluminescent signal was equal to or lower than background radiance, was modestly—albeit statistically significantly—extended for IL13-producing MSCs following IM implantation (Fig. 7B, 7C). This was also true following IC implantation, with an even more pronounced graft survival-promoting effect of IL13 in these animals (Fig. 7E, 7F). In conclusion, these data illustrate that IL13 can delay the course of allograft rejection in both muscle and brain tissue.

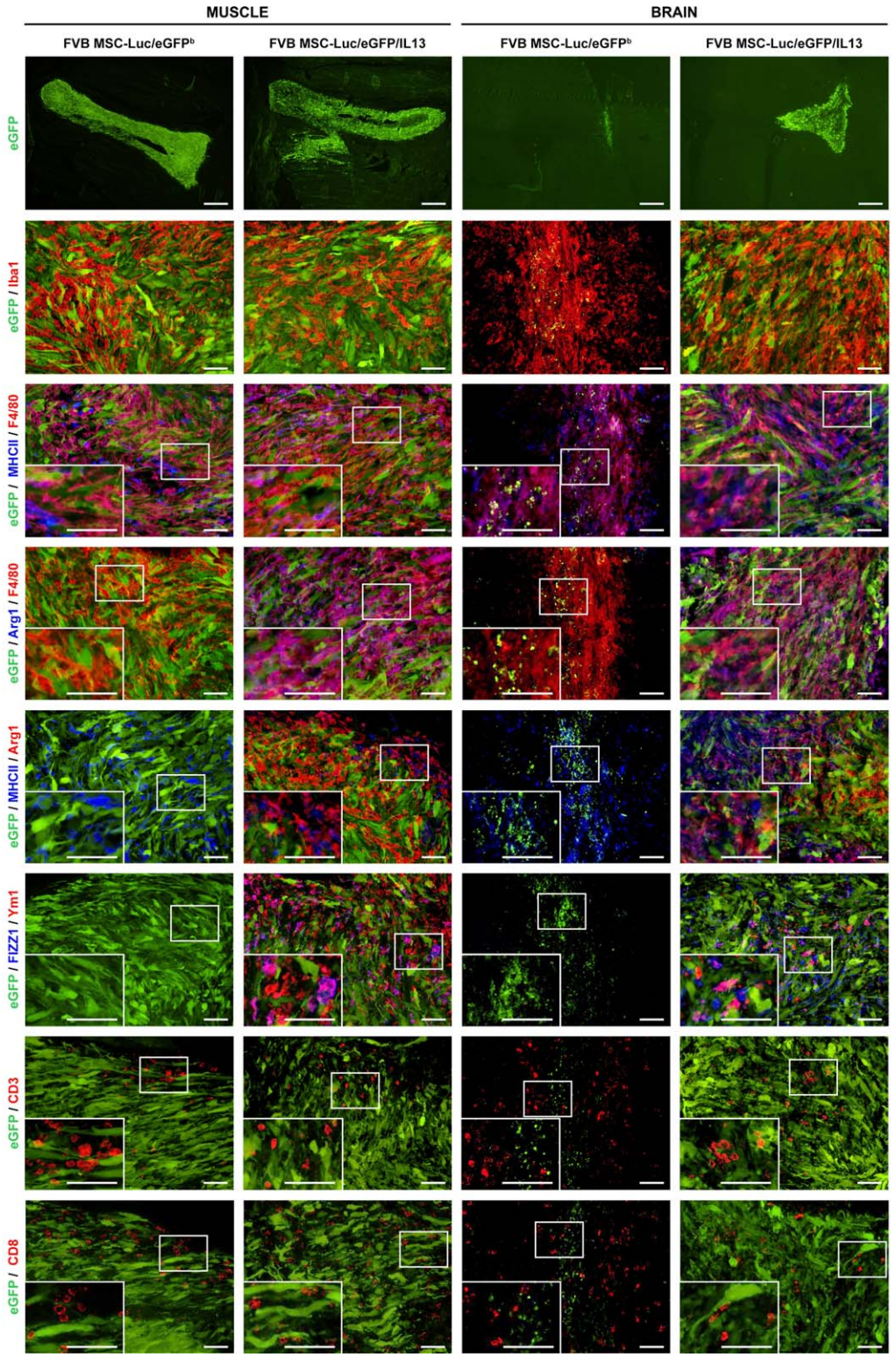

Figure 5. Transplantation of IL13-producing MSCs induces an alternatively activated phenotype in graft-infiltrating macrophages (and microglia). Representative immunofluorescence images of FVB MSC-Luc/eGFP^{b} and FVB MSC-Luc/eGFP/IL13 implants in muscle (5 days postgrafting) or brain (7 days postgrafting) of C57BL/6 mice ($n = 5$/condition). Iba1 and F4/80 were used as general macrophage/microglia markers, MHCII as a typical activation marker, and Arg1, Ym1, and FIZZ1 as markers of alternative M2a activation. In addition, graft sites were evaluated for the presence of $CD3^{+}$ and $CD8^{+}$ T cells. Secondary antibodies were coupled to Alexa Fluor 555 for red fluorescence, Alexa Fluor 350 for blue fluorescence or Cy5 for far red fluorescence (for the F4/80 + MHCII double staining, MHCII was stained in far red, but is represented here in blue). Images were acquired using the ×4 (top row) and ×20 (other rows, both main images and insets) objective lenses. Scale bars = 500 μm in the top row and 50 μm in all other images (both main images and insets). Abbreviations: eGFP, enhanced green fluorescent protein; IL, interleukin; MHC, major histocompatibility complex; MSC, mesenchymal stem cell.

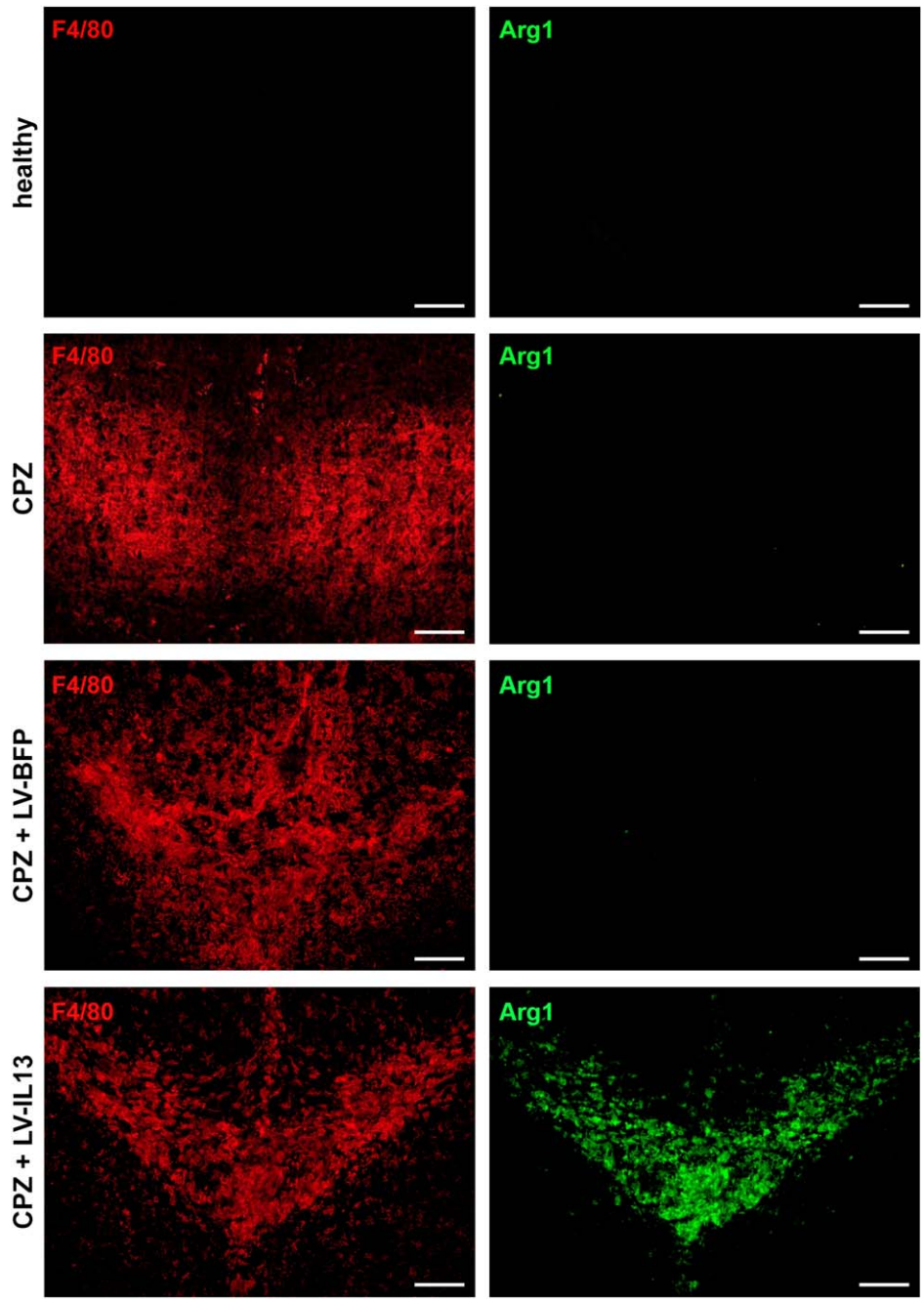

Figure 6. IL13 alone is sufficient to induce in vivo M2a macrophage/microglia polarization. Representative immunofluorescence images are shown of the splenium of the corpus callosum of healthy control mice (healthy, $n = 5$), CPZ-fed noninjected control mice (CPZ, $n = 5$), CPZ-fed pCHMWS-BFP-IRES-Pac LV injected mice (CPZ + LV-BFP, $n = 6$), and CPZ-fed pCHMWS-mIL13-IRES-Pac LV injected mice (CPZ + LV-IL13, $n = 6$) after 4 weeks of CPZ diet. F4/80 was used as general macrophage/microglia marker and Arg1 as a marker of alternative M2a activation. Secondary antibodies were coupled to Alexa Fluor 555 for red fluorescence (F4/80) or Alexa Fluor 350 for blue fluorescence (Arg1, depicted here in green). Images were acquired using the ×20 objective lens and scale bars = 100 μm. Abbreviations: BFP, blue fluorescent protein; CPZ, cuprizone; IL, interleukin; LV, lentiviral vector.

Discussion

To this day, immune recognition of allografts remains the major hurdle in achieving successful allogeneic cell transplantation, and thus, sustained therapeutic benefit of allogeneic cellular therapies. Correspondingly, we observed that transplantation of MSCs, cells with an established in vitro immunomodulatory potential [28–30], into allogeneic hosts irrevocably resulted in allograft rejection. Furthermore, IM MSC transplantation triggered the induction of graft-specific $CD8^+$ T cells in allogeneic hosts. Alloreactive T cells can be sensitized via three distinct pathways: direct, indirect, and semidirect allorecognition [62, 63]. Following in vitro IFNγ stimulation, MSCs have been found to upregulate MHCII expression and display some antigen-presenting properties in the context of direct allorecognition [64]. Histological analysis of the graft sites however did not

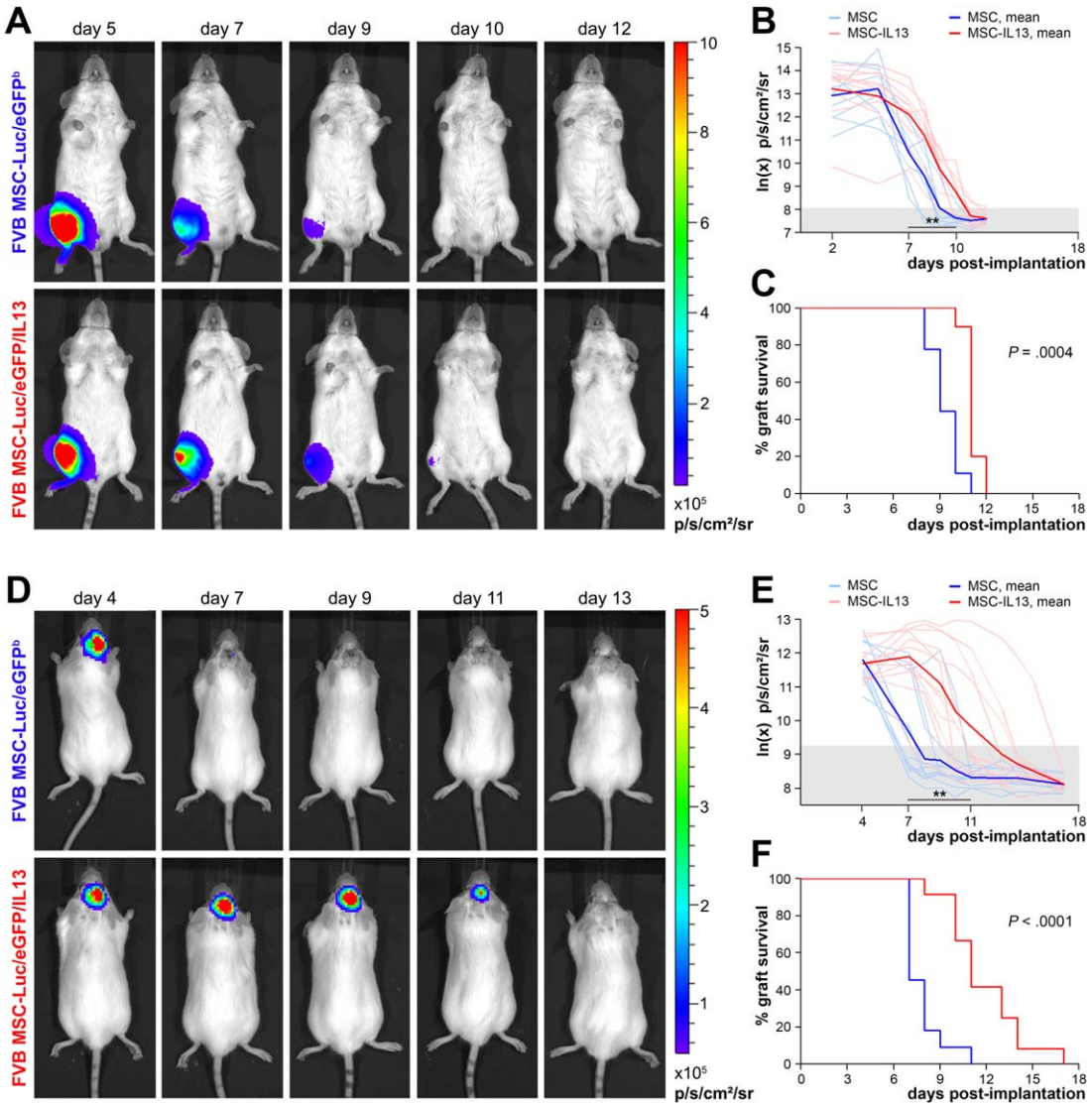

Figure 7. IL13 prolongs MSC allograft survival upon both intramuscular (IM) and intracranial (IC) administration. **(A, D)**: In vivo bioluminescence imaging (BLI) of FVB MSCs-Luc/eGFP^b and FVB MSCs-Luc/eGFP/IL13 following IM (A) or IC (D) transplantation in albino C57BL/6 mice. Representative time course images are shown. The most intense bioluminescence signal is shown in red, the weakest in blue. Light intensity is presented as the average number of photons per second per square centimeter per steradian. **(B, E)**: Quantitative analysis of in vivo BLI measurements of IM (B) or IC (E) FVB MSC-Luc/eGFP^b (MSC, muscle: $n = 8$ and brain: $n = 10$) or FVB MSC-Luc/eGFP/IL13 (MSC-IL13, muscle: $n = 9$ and brain: $n = 11$) allografts in albino C57BL/6 mice. Light emission was measured from a fixed region of interest, and measured BLI signals (expressed as ln(x)-transformed photons/second/cm^2/steradian) are provided longitudinally for each mouse analyzed. The bold blue and red lines indicate the average logarithmic BLI signals of FVB MSC-Luc/eGFP^b and FVB MSC-Luc/eGFP/IL13 allografts, respectively. Background radiance is demarcated by the gray area. **, $p < .01$ **(C, F)**: Cumulative survival of FVB MSC-Luc/eGFP^b (blue) and FVB MSC-Luc/eGFP/IL13 (red) allografts following IM (C) or IC (F) implantation into albino C57BL/6 mice. Abbreviations: eGFP, enhanced green fluorescent protein; IL, interleukin; MSC, mesenchymal stem cell.

reveal MHCII expression by grafted MSCs in vivo (Fig. 5, third and fifth rows). In contrast, indirect allorecognition of MSCs is likely to occur, albeit at a slower rate, accounting for only <10% of the alloreactive T cell repertoire during acute rejection [65]. Particularly in the case of fully MHC-mismatched cell grafts, this process will require a more complex sequence of events to achieve effective allograft elimination [66]. Consequently, we believe that the semidirect pathway of allorecognition is the most likely mechanism to explain the rapid induction of allograft-specific T cell responses following transplantation of fully MHC-mismatched MSCs [62]. Furthermore, there is compelling evidence that innate immune cells are also capable to distinguish between self and allogeneic non-self [67, 68]. Since the transplanted cells used in this study were fully incompatible with their recipients, it is likely that multiple allorecognition mechanisms jointly contributed to the observed allograft rejection.

In our opinion, distinct allograft recognition mechanisms may be responsible for the rejection of IM and IC allografts, illustrated by their differential capacity to induce alloreactive T cells. Even so, histological analysis revealed the presence of CD8$^+$ T cells in both IM and IC allografts. Given the absence of alloreactive T cells in secondary lymphoid organs after IC transplantation of allogeneic MSCs, it is safe to assume that CD8$^+$ T

cells found in IC allografts are not allograft-specific. The antigen-specificity of IM allograft-infiltrating $CD8^+$ T cells however remains to be established. This was not examined here as graft-infiltrating T cells were scarce, impeding the isolation of sufficient T cells for flow cytometric analysis. The involvement of T cells in MSC allograft rejection was previously demonstrated by Zangi et al. [33], as they found that intraperitoneal MSC allografts survived in BALB/c nude mice but not in fully competent BALB/c recipients. Consequently, it is expected that at least some of the T cells infiltrating IM allografts are alloreactive and actively contribute to allograft rejection.

The ultimate goal of our study was to modulate these existing allorecognition mechanisms in vivo, in favor of MSC allograft survival. Upon transduction with an IL13-expressing LV, we found that local IL13 production by MSC allografts induced an alternatively activated phenotype in graft-infiltrating macrophages (and microglia). Although macrophages can adopt a myriad of distinct phenotypes in response to different stimuli, nonresting macrophages are generally classified as either "classically" (M1) or "alternatively" (M2) activated. MHCII is typically upregulated upon macrophage activation (in both M1- and M2-oriented cells), whereas additional expression of the enzymes Arg1, Ym1, and FIZZ1 is indicative of the M2a phenotype [46, 60]. In our study, induction of the M2a macrophage/microglia phenotype was a direct effect of MSC-derived IL13, as IC injection of an IL13-encoding LV into inflammatory CNS lesions was similarly found to induce Arg1 expression in macrophages/microglia (Fig. 6). Furthermore, we report that this IL13-driven shift in macrophage (and microglia) phenotype coincides with reduced peripheral T cell responses following IM transplantation of allogeneic MSCs. Interestingly, elevated Arg1 expression by macrophages has previously been associated with decreased T cell function [69, 70]. Rodriguez and colleagues found that macrophages stimulated with IL4 + IL13 upregulated their expression of Arg1 and cationic amino acid transporter 2B, causing a rapid drop in extracellular L-arginine levels. Due to this depletion, CD3ζ chain expression was lost on activated T cells, resulting in impaired T cell proliferation and decreased cytokine production. Similarly, we postulate that IL13-induced M2a macrophages migrate to secondary lymphoid organs—to exert their role as APCs—where they locally deplete the environment of L-arginine and cause impaired T cell function, thus recapitulating our flow cytometry results (Fig. 4A, 4B, 4E, 4F). Alternatively, M2a macrophages might display a reduced migratory capacity towards secondary lymphoid organs, and/or IL13-conditioned M2a macrophages (and microglia) might display a reduction in innate effector functions (such as direct allograft killing), although these hypotheses remain to be investigated. Nevertheless, we postulate that MSC allograft rejection is predominantly mediated by the direct action of macrophages (and microglia). In the case of IM MSC transplantation, the allograft rejection process may additionally be aided by alloreactive T cells. But regardless of the relative contributions of these different allorecognition mechanisms, it is evident that IL13 has the potential to modulate both innate and adaptive immune mechanisms, ultimately resulting in extended MSC allograft survival.

When considering possible applications of IL13-overexpressing MSCs, one should take into account that allograft-survival was only modestly prolonged by MSC-derived IL13. Although this excludes applications in which sustained MSC survival is recommended, for example, long-term production of therapeutic proteins such as erythropoietin or factor VIII [71, 72], models which predominantly rely on the supportive and regenerative functions of MSCs for disease improvement may still benefit from a slightly extended therapeutic window of allogeneic MSC grafts. For example, the beneficial effects of allogeneic MSCs in ischemic stroke were still apparent 14 days after cell administration, even though just a fraction of transplanted cells is expected to persist at this point [37]. It is therefore safe to assume that a prolongation of the grafted MSCs' therapeutic period will go hand in hand with an improved therapeutic outcome.

Conclusion

In conclusion, this study demonstrates that locally secreted IL13 modulates allograft-specific immunity by promoting the M2a activation state in graft-infiltrating macrophages and by limiting the induction of allograft-specific $CD8^+$ T cell responses. This IL13-mediated modulation resulted in a prolongation of allogeneic MSC survival in both muscle and brain tissue. Aside from transplantation research, the pleiotropic effects IL13 further encourage the application of this cytokine for the relief of acute or chronic inflammation in models of trauma or disease.

Acknowledgments

We thank A. Liston and S. Humblet-Baron (VIB Translational Immunology Lab, KU Leuven, Belgium) for sharing their optimized staining protocols for intracellular cytokine analysis by flow cytometry. This work was supported by research grants G.0130.11 and G.0136.11 (granted to A.V.d.L., Z.N.B. and P.P.), G.0131.11 (granted to Z.N.B. and P.P.), G.0834.11 (granted to S.H. and P.P.) and G.0851.11 (granted to C.V. and Z.N.B.) of the Research Foundation Flanders (FWO Vlaanderen, Belgium) and in part by a Methusalem research grant from the Flemish government (granted to H.G.). C.J.H. and E.Lu. hold a PhD studentship from the FWO Vlaanderen. C.G. and D.L.B. hold a PhD studentship from the Flemish Institute for Science and Technology (IWT Vlaanderen).

Author Contributions

C.J.H.: conception and design, collection and/or assembly of data, data analysis and interpretation, and manuscript writing; E.L.: collection and/or assembly of data and data analysis and interpretation; K.R., D.L.B., N.D.V., and C.G.: conception and design, collection and/or assembly of data, and data analysis and interpretation; M.D., L.V., and A.Q.: collection and/or assembly of data; D.D.: conception and design and data analysis and interpretation; E.F.: data analysis and interpretation; J.D.: collection and/or assembly of data and administrative support;: E.L. and V.D.R.: conception and design and data analysis and interpretation; H.G., A.V.d.L., Z.N.B., and C.V.: conception and design and financial support; S.H.: conception and design, data analysis and interpretation, and financial support; M.M.: conception and design and provision of study material; P.P.: conception and design, data analysis and interpretation, financial support, manuscript writing, and final approval of manuscript.

Disclosure of Potential Conflicts of Interest

The authors indicate no potential conflicts of interest.

References

1 Friedenstein AJ, Gorskaja JF, Kulagina NN. Fibroblast precursors in normal and irradiated mouse hematopoietic organs. Exp Hematol 1976;4:267–274.

2 Horwitz EM, Prockop DJ, Fitzpatrick LA et al. Transplantability and therapeutic effects of bone marrow-derived mesenchymal cells in children with osteogenesis imperfecta. Nat Med 1999;5:309–313.

3 Arinzeh TL, Peter SJ, Archambault MP et al. Allogeneic mesenchymal stem cells regenerate bone in a critical-sized canine segmental defect. J Bone Joint Surg Am 2003;85:1927–1935.

4 Quevedo HC, Hatzistergos KE, Oskouei BN et al. Allogeneic mesenchymal stem cells restore cardiac function in chronic ischemic cardiomyopathy via trilineage differentiating capacity. Proc Natl Acad Sci USA 2009;106:14022–14027.

5 Sun L, Akiyama K, Zhang H et al. Mesenchymal stem cell transplantation reverses multiorgan dysfunction in systemic lupus erythematosus mice and humans. Stem Cells 2009;27:1421–1432.

6 Chen FH, Rousche KT, Tuan RS. Technology Insight: Adult stem cells in cartilage regeneration and tissue engineering. Nat Clin Pract Rheum 2006;2:373–382.

7 Cristofanilli M, Harris VK, Zigelbaum A et al. Mesenchymal stem cells enhance the engraftment and myelinating ability of allogeneic oligodendrocyte progenitors in dysmyelinated mice. Stem Cells Dev 2011;20:2065–2076.

8 Uccelli A, Moretta L, Pistoia V. Immunoregulatory function of mesenchymal stem cells. Eur J Immunol 2006;36:2566–2573.

9 Nauta AJ, Fibbe WE. Immunomodulatory properties of mesenchymal stromal cells. Blood 2007;110:3499–3506.

10 Casiraghi F, Azzollini N, Cassis P et al. Pretransplant infusion of mesenchymal stem cells prolongs the survival of a semiallogeneic heart transplant through the generation of regulatory T cells. J Immunol 2008;181:3933–3946.

11 Jiang X, Liu C, Hao J et al. CD4+CD25+ regulatory T cells are not required for mesenchymal stem cell function in fully MHC-mismatched mouse cardiac transplantation. Cell Tissue Res 2014;358:503–514.

12 Tan J, Wu W, Xu X et al. Induction therapy with autologous mesenchymal stem cells in living-related kidney transplants: A randomized controlled trial. JAMA 2012;307:1169–1177.

13 Le Blanc K, Frassoni F, Ball L et al. Mesenchymal stem cells for treatment of steroid-resistant, severe, acute graft-versus-host disease: A phase II study. Lancet 2008;371:1579–1586.

14 Connick P, Kolappan M, Crawley C et al. Autologous mesenchymal stem cells for the treatment of secondary progressive multiple sclerosis: An open-label phase 2a proof-of-concept study. Lancet Neurol 2012;11:150–156.

15 Schwarz EJ, Alexander GM, Prockop DJ et al. Multipotential marrow stromal cells transduced to produce L-DOPA: Engraftment in a rat model of Parkinson disease. Hum Gene Ther 1999;10:2539–2549.

16 Li Y, Chen J, Zhang CL et al. Gliosis and brain remodeling after treatment of stroke in rats with marrow stromal cells. Glia 2005;49:407–417.

17 Ronsyn MW, Daans J, Spaepen G et al. Plasmid-based genetic modification of human bone marrow-derived stromal cells: Analysis of cell survival and transgene expression after transplantation in rat spinal cord. BMC Biotechnol 2007;7:1–17.

18 Caplan AI, Dennis JE. Mesenchymal stem cells as trophic mediators. J Cell Biochem 2006;98:1076–1084.

19 Wu Y, Chen L, Scott PG et al. Mesenchymal stem cells enhance wound healing through differentiation and angiogenesis. Stem Cells 2007;25:2648–2659.

20 Eliopoulos N, Al-Khaldi A, Crosato M et al. A neovascularized organoid derived from retrovirally engineered bone marrow stroma leads to prolonged in vivo systemic delivery of erythropoietin in nonmyeloablated, immunocompetent mice. Gene Ther 2003;10:478–489.

21 Van Damme A, Chuah MK, Dell'accio F et al. Bone marrow mesenchymal cells for haemophilia A gene therapy using retroviral vectors with modified long-terminal repeats. Haemophilia 2003;9:94–103.

22 Lee RH, Pulin AA, Seo MJ et al. Intravenous hMSCs improve myocardial infarction in mice because cells embolized in lung are activated to secrete the anti-inflammatory protein TSG-6. Cell Stem Cell 2009;5:54–63.

23 Figueroa FE, Carrión F, Villanueva S et al. Mesenchymal stem cell treatment for autoimmune diseases: A critical review. Biol Res 2012;45:269–277.

24 Ankrum J, Karp JM. Mesenchymal stem cell therapy: Two steps forward, one step back. Trends Mol Med 2010;16:203–209.

25 Ankrum JA, Ong JF, Karp JM. Mesenchymal stem cells: Immune evasive, not immune privileged. Nat Biotechnol 2014;32:252–260.

26 Caplan AI. Why are MSCs therapeutic?. New data: New insight. J Pathol 2009;217:318–324.

27 Shen J, Tsai YT, Dimarco NM et al. Transplantation of mesenchymal stem cells from young donors delays aging in mice. Sci Rep 2011;1:67.

28 Di Nicola M, Carlo-Stella C, Magni M et al. Human bone marrow stromal cells suppress T-lymphocyte proliferation induced by cellular or nonspecific mitogenic stimuli. Blood 2002;99:3838–3843.

29 Krampera M, Glennie S, Dyson J et al. Bone marrow mesenchymal stem cells inhibit the response of naive and memory antigen-specific T cells to their cognate peptide. Blood 2003;101:3722–3729.

30 Beyth S, Borovsky Z, Mevorach D et al. Human mesenchymal stem cells alter antigen-presenting cell maturation and induce T-cell unresponsiveness. Blood 2005;105:2214–2219.

31 Djouad F, Plence P, Bony C et al. Immunosuppressive effect of mesenchymal stem cells favors tumor growth in allogeneic animals. Blood 2003;102:3837–3844.

32 De Vocht N, Praet J, Reekmans K et al. Tackling the physiological barriers for successful mesenchymal stem cell transplantation into the central nervous system. Stem Cell Res Ther 2013;4:101.

33 Zangi L, Margalit R, Reich-Zeliger S et al. Direct imaging of immune rejection and memory induction by allogeneic mesenchymal stromal cells. Stem Cells 2009;27:2865–2874.

34 Eggenhofer E, Benseler V, Kroemer A et al. Mesenchymal stem cells are short-lived and do not migrate beyond the lungs after intravenous infusion. Front Immunol 2012;3:297.

35 Harting MT, Jimenez F, Xue H et al. Intravenous mesenchymal stem cell therapy for traumatic brain injury. J Neurosurg 2009;110:1189–1197.

36 Ezquer FE, Ezquer ME, Parrau DB et al. Systemic administration of multipotent mesenchymal stromal cells reverts hyperglycemia and prevents nephropathy in type 1 diabetic mice. Biol Blood Marrow Transplant 2008;14:631–640.

37 Gutierrez-Fernandez M, Rodriguez-Frutos B, Ramos-Cejudo J et al. Effects of intravenous administration of allogenic bone marrow- and adipose tissue-derived mesenchymal stem cells on functional recovery and brain repair markers in experimental ischemic stroke. Stem Cell Res Ther 2013;4:11.

38 Everaert BR, Bergwerf I, De Vocht N et al. Multimodal in vivo imaging reveals limited allograft survival, intrapulmonary cell trapping and minimal evidence for ischemia-directed BMSC homing. BMC Biotechnol 2012;12:93.

39 Quertainmont R, Cantinieaux D, Botman O et al. Mesenchymal stem cell graft improves recovery after spinal cord injury in adult rats through neurotrophic and pro-angiogenic actions. PloS One 2012;7:e39500.

40 Ishikane S, Ohnishi S, Yamahara K et al. Allogeneic injection of fetal membrane-derived mesenchymal stem cells induces therapeutic angiogenesis in a rat model of hind limb ischemia. Stem Cells 2008;26:2625–2633.

41 Chen J, Li Y, Wang L et al. Therapeutic benefit of intravenous administration of bone marrow stromal cells after cerebral ischemia in rats. Stroke 2001;32:1005–1011.

42 Eliopoulos N, Stagg J, Lejeune L et al. Allogeneic marrow stromal cells are immune rejected by MHC class I- and class II-mismatched recipient mice. Blood 2005;106:4057–4065.

43 Nauta AJ, Westerhuis G, Kruisselbrink AB et al. Donor-derived mesenchymal stem cells are immunogenic in an allogeneic host and stimulate donor graft rejection in a nonmyeloablative setting. Blood 2006;108:2114–2120.

44 Sbano P, Cuccia A, Mazzanti B et al. Use of donor bone marrow mesenchymal stem cells for treatment of skin allograft rejection in a preclinical rat model. Arch Dermatol Res 2008;300:115–124.

45 Tambuyzer BR, Bergwerf I, De Vocht N et al. Allogeneic stromal cell implantation in brain tissue leads to robust microglial activation. Immunol Cell Biol 2009;87:267–273.

46 Van Dyken SJ, Locksley RM. Interleukin-4- and interleukin-13-mediated alternatively activated macrophages: Roles in homeostasis and disease. Annu Rev Immunol 2013;31:317–343.

47 Graber P, Gretener D, Herren S et al. The distribution of IL-13 receptor α1 expression on B cells, T cells and monocytes and its regulation by IL-13 and IL-4. Eur J Immunol 1998;28:4286–4298.
48 de Vries JE. The role of IL-13 and its receptor in allergy and inflammatory responses. J Allergy Clin Immunol 102:165–169.
49 Bergwerf I, De Vocht N, Tambuyzer B et al. Reporter gene-expressing bone marrow-derived stromal cells are immunetolerated following implantation in the central nervous system of syngeneic immunocompetent mice. BMC Biotechnol 2009;9:1.
50 Ibrahimi A, Vande Velde G, Reumers V et al. Highly efficient multicistronic lentiviral vectors with peptide 2A sequences. Hum Gene Ther 2009;20:845–860.
51 Baekelandt V, Eggermont K, Michiels M et al. Optimized lentiviral vector production and purification procedure prevents immune response after transduction of mouse brain. Gene Ther 2003;10:1933–1940.
52 Geraerts M, Michiels M, Baekelandt V et al. Upscaling of lentiviral vector production by tangential flow filtration. J Gene Med 2005;7:1299–1310.
53 Praet J, Santermans E, Reekmans K et al. Histological characterization and quantification of cellular events following neural and fibroblast(-like) stem cell grafting in healthy and demyelinated CNS tissue. In: Christ B, Oerlecke J, Stock P, eds. Animal Models for Stem Cell Therapy. New York: Springer; 2014:265–283.
54 De Vocht N, Lin D, Praet J et al. Quantitative and phenotypic analysis of mesenchymal stromal cell graft survival and recognition by microglia and astrocytes in mouse brain. Immunobiology 2013;218:696–705.
55 Le Blon D, Hoornaert C, Daans J et al. Distinct spatial distribution of microglia and macrophages following mesenchymal stem cell implantation in mouse brain. Immunol Cell Biol 2014;92:650–658.
56 Guglielmetti C, Praet J, Rangarajan JR et al. Multimodal imaging of subventricular zone neural stem/progenitor cells in the cuprizone mouse model reveals increased neurogenic potential for the olfactory bulb pathway, but no contribution to remyelination of the corpus callosum. NeuroImage 2014;86:99–110.
57 Orije J, Kara F, Guglielmetti C et al. Longitudinal monitoring of metabolic alterations in cuprizone mouse model of multiple sclerosis using 1H-magnetic resonance spectroscopy. NeuroImage 2015;114:128–135.
58 Praet J, Orije J, Kara F et al. Cuprizone-induced demyelination and demyelination-associated inflammation result in different proton magnetic resonance metabolite spectra. NMR Biomed 2015;28:505–513.
59 Praet J, Reekmans K, Lin D et al. Cell type-associated differences in migration, survival, and immunogenicity following grafting in CNS tissue. Cell Transplant 2012;21:1867–1881.
60 Mantovani A, Sica A, Sozzani S et al. The chemokine system in diverse forms of macrophage activation and polarization. Trends Immunol 2004;25:677–686.
61 Praet J, Guglielmetti C, Berneman Z et al. Cellular and molecular neuropathology of the cuprizone mouse model: Clinical relevance for multiple sclerosis. Neurosci Biobehav R 2014;47:485–505.
62 Herrera OB, Golshayan D, Tibbott R et al. A novel pathway of alloantigen presentation by dendritic cells. J Immunol 2004; 173:4828–4837.
63 Sivanathan KN, Gronthos S, Rojas-Canales D et al. Interferon-gamma modification of mesenchymal stem cells: Implications of autologous and allogeneic mesenchymal stem cell therapy in allotransplantation. Stem Cell Rev 2014;10:351–375.
64 Chan JL, Tang KC, Patel AP et al. Antigen-presenting property of mesenchymal stem cells occurs during a narrow window at low levels of interferon-gamma. Blood 2006; 107:4817–4824.
65 Benichou G, Valujskikh A, Heeger PS. Contributions of direct and indirect T cell alloreactivity during allograft rejection in mice. J Immunol 1999;162:352–358.
66 Lee RS, Grusby MJ, Glimcher LH et al. Indirect recognition by helper cells can induce donor-specific cytotoxic T lymphocytes in vivo. J Exp Med 1994;179:865–872.
67 Zecher D, van Rooijen N, Rothstein DM et al. An innate response to allogeneic nonself mediated by monocytes. J Immunol 2009;183:7810–7816.
68 Liu W, Xiao X, Demirci G et al. Innate NK cells and macrophages recognize and reject allogeneic nonself in vivo via different mechanisms. J Immunol 2012;188:2703–2711.
69 Rodriguez PC, Zea AH, DeSalvo J et al. L-arginine consumption by macrophages modulates the expression of CD3 zeta chain in T lymphocytes. J Immunol 2003;171:1232–1239.
70 Bronte V, Serafini P, Mazzoni A et al. L-arginine metabolism in myeloid cells controls T-lymphocyte functions. Trends Immunol 2003;24:301–305.
71 Campeau PM, Rafei M, Francois M et al. Mesenchymal stromal cells engineered to express erythropoietin induce anti-erythropoietin antibodies and anemia in allorecipients. Mol Ther 2009;17:369–372.
72 Lillicrap D, VandenDriessche T, High K. Cellular and genetic therapies for haemophilia. Haemophilia 2006;12 (Suppl 3):36–41.


See www.StemCells.com for supporting information available online.

